

# PHYSICAL REVIEW LETTERS

VOLUME 31

19 NOVEMBER 1973

NUMBER 21

## Monoelectron Oscillator

D. Wineland, P. Ekstrom, and H. Dehmelt

*Department of Physics, University of Washington, Seattle, Washington 98195*

(Received 13 August 1973)

A single electron has been isolated in a  $\sim 6$ -V-deep Penning trap. Using synchronous detection its forced axial oscillation at 55.7 MHz has been observed continuously. Excitation was either sideband at 54.7 MHz or parametric at 111.4 MHz, the latter making collision-induced  $180^\circ$  phase jumps visible. The monoelectron oscillator is profitably looked upon as a fixed-in-space pseudoatom, free of first- and second-order Doppler shifts.

The development of techniques for the permanent containment of a single charged particle in a parabolic potential well formed by suitable electromagnetic fields in high vacuum, and its thermalization/refrigeration and continuous non-destructive detection by electromagnetic interaction with an  $LC$  circuit, appears rewarding for several reasons.<sup>1</sup> One of them, which provided the immediate impetus for the present study,<sup>2</sup> is the elimination of space-charge shifts<sup>3</sup> in free-electron or -positron  $g-2$  experiments<sup>4</sup> currently in preparation in this laboratory. The same consideration also applies to charge/mass measurements in general. Another noteworthy point is the small size of the orbit which minimizes field homogeneity problems; e.g., in the experiments on an  $80^\circ\text{K}$  electron to be described, the cyclotron orbit diameter is  $\sim 1\ \mu\text{m}$  while the axial extension of the orbit is  $\sim 200\ \mu\text{m}$ . In view of the foregoing it becomes profitable to look upon the monoelectron oscillator as a fixed-in-space pseudoatom free of first- and second-order Doppler shifts, whose various energy levels are accessible both experimentally and theoretically to great accuracy. In fields large enough or of sufficient controlled inhomogeneity these levels are only approximately equidistant.

The following principle underlies our experi-

mental approach for isolating a single electron and observing its axial oscillation in a Penning trap.<sup>1,5</sup> While for a sample of many electrons colliding with each other and the residual gas, even off-resonance excitation leads to energy absorption by the electron gas accompanied by rapid increase of its temperature and loss of the sample, for a *single* electron in a perfect vacuum continuous detection *without* any energy absorption by the electron becomes possible by observing the out-of-phase current induced by its driven motion in the external circuit.

The differential equation describing an elastically bound electron of resonance frequency  $\nu_{z0}$  located between two parallel capacitor plates of separation  $d$  driven by an rf potential  $u_d$  at  $\nu_z' \simeq \nu_{z0}$  is quite analogous to that of a series-resonant circuit of inductance  $l_1$  and capacity  $c$ , with  $l_1 c \omega_{z0}^2 = 1$ , which connects the plates. Here  $l_1$  is given by  $l_1 = m d^2 / e^2$  with  $m$  the electron mass. (Throughout the paper we use  $\omega/2\pi$  and  $\nu$  interchangeably, i.e.,  $\omega_{z0}/2\pi \equiv \nu_{z0}$ ,  $\omega_z'/2\pi \equiv \nu_z'$ , etc.) If the electron is inside a Penning trap near its center,  $e$  must be replaced by an effective charge  $\sim \frac{1}{2}e$  since only about  $\frac{1}{2}$  of the field lines emanating from the electron end on the end caps, yielding  $l_1 \simeq 16 m z_0^2 / e^2$ , the cap separation  $2z_0 \simeq 7.6$  mm taking the place of  $d$ . In view of the forego-

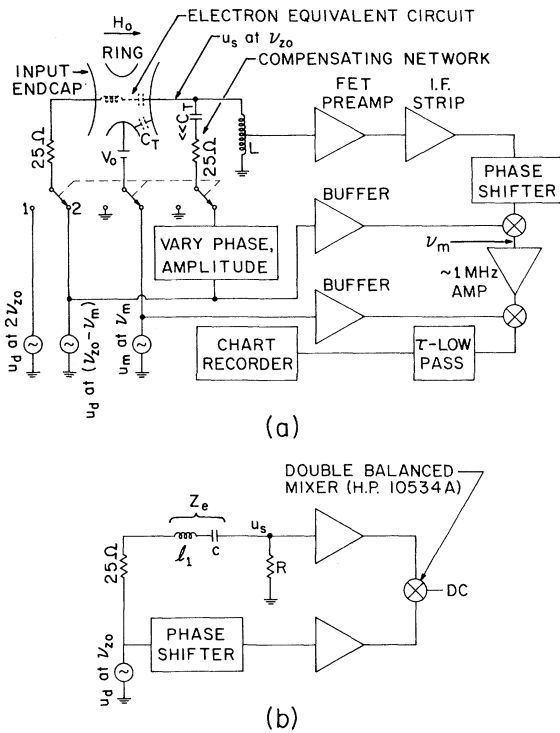


FIG. 1. Apparatus for isolating and continuously observing the forced oscillation of a single elastically bound electron. A block diagram is given in (a). Switch position 2 is for direct excitation, position 1 for parametric excitation of the forced oscillation at  $\nu_{z0} \approx 55.7$  MHz. In (b) an equivalent circuit is shown for switch position 2,  $Z_e$  representing the electron.

ing, the elastically bound electron near its resonant frequency  $\nu_{z0}$  will present a pure imaginary impedance  $Z_e \approx 2j(\omega_z' - \omega_{z0})l_1$ . However, this formula holds strictly only in the limit of vanishing drive  $u_d$  because the trap is slightly anharmonic and the electron resonance frequency  $\nu_z$  is shifted from  $\nu_{z0}$  by an amount proportional to the  $u_d$ -dependent total average axial oscillatory energy  $W_1$ , with  $d\nu_z/dW_1 \approx +40$  kHz/eV for the current trap. The forced axial  $z$  motion of the electron(s) at the frequency  $\nu_z' \approx \nu_{z0} = 55.7$  MHz is now observed in the manner shown in Fig. 1(a), where  $V_0 \approx +12$  V,  $H_0 \approx 4000$  G. Residual gas pressure was  $\sim 10^{-11}$  Torr; LC circuit temperature,  $\sim 80^\circ\text{K}$ . A  $25\text{-}\Omega$  source  $u_d$  drives the input end cap at  $\nu_z'$  near the zero-amplitude frequency  $\nu_{z0}$ . The output end cap is connected to the LC tank circuit,  $C \approx C_T \approx 10$  pF, of shunt impedance  $R \approx 100$  k $\Omega$ , parallel resonant at  $\nu_{z0}$ . The end cap-end cap capacity was canceled out as in the analogous crystal-filter circuit by the compensat-

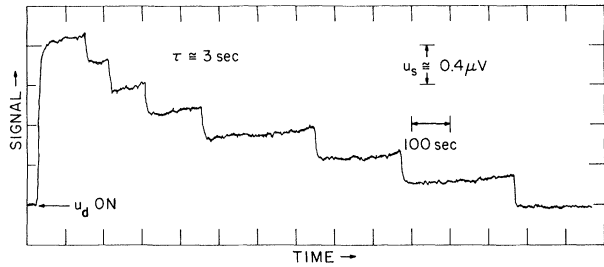


FIG. 2. Recorder trace of forced-oscillation signal versus time. The signal at  $\nu_{z0} \approx 55.7$  MHz for an initially injected bunch of electrons decreases discontinuously as the electrons are successively boiled out of the trap by the drive at  $\nu_z' \approx 54.7$  MHz. The last plateau corresponds to a single electron.

ing network. For finite  $u_d$  and  $W_1$ , and when for reasons of experimental convenience we now choose the drive frequency  $\nu_z' = \nu_{z0}$ , the single electron presents an impedance  $Z_e \approx -2j\Delta l_1$  with  $\Delta \equiv (d\omega_z/dW_1)W_1$ ,  $l_1 \approx 8000$  H, and  $|Z_e| \gg R$ . Electrically, the apparatus is equivalent to Fig. 1(b). The resulting current  $i_d \approx ju_d/2\Delta l_1$  develops a signal  $u_s = i_d R$  which is amplified and then mixed with the drive signal to give a dc output in a Hewlett-Packard 10534A balanced mixer.

In practice, the above procedure could not be used directly because of spurious signals caused by acoustic modulation of the incompletely canceled carrier, etc. Instead the electron frequency was modulated at  $\nu_m \approx 1$  MHz by applying an rf voltage  $u_m$  to the ring (modulation index  $\approx 0.6$ ).<sup>5</sup> The drive voltage was applied to the lower sideband (at  $\nu_{z0} - \nu_m = 54.7$  MHz) and the resulting carrier signal at 55.7 MHz detected as shown in Fig. 1(a). (Raising  $\nu_m$  to  $\sim 10$  MHz has eliminated the need for the compensation network in the meantime.) In a typical experiment, approximately ten electrons were loaded into the trap by knocking off slow electrons from the residual gas with an electron beam using a filling time which was scaled down linearly from the time needed to load a large, easily measurable number.<sup>7</sup> A threshold value of  $u_d$  was then applied which presumably gave the electrons sufficient energy such that gas collisions would occasionally transfer back enough random energy from the  $x$ - $y$  motion to the  $z$  motion to cause an electron to strike the end caps and be lost. In this way electrons could be expelled from the trap at a controlled rate, yielding recorder traces of the output voltage versus time as shown in Fig. 2. The features of the last few "steps" are quite reproducible; the last

step, which we attribute to one electron, corresponds to an axial energy  $W_1 \cong 0.2$  eV as determined from a calibration of the signal strength  $u_s$  against the shot-noise voltage produced by the filament nearest the output end cap.<sup>5</sup> Much longer observation periods<sup>5</sup> (weeks) are possible for reduced values of  $u_d$ . The success of the experiment depends crucially on a favorable ratio of the  $z$ -motion damping time  $t_{zt}$  to the mean interval between electron-residual-gas collisions  $T_r$ ,  $t_{zt}/T_r \ll 1$ . For  $t_{zt}/T_r \gg 1$ , the random excitation of the free oscillation quickly reaches such occasional magnitudes that the electrons hit one of the caps even for weak drive  $u_d$  (and weak signal  $u_s$ ). In the current work  $t_{zt} = l_1/R = 0.1$  sec,  $T_r \cong 10$  sec, and  $t_{zt}/T_r \cong 0.01$  were attained.

In addition, we have also observed the behavior characteristic of a single electron under parametric excitation<sup>8</sup> at  $2\nu_{z0}$ , the detection circuit remaining the same. In this case, because the phase<sup>1</sup> of the driven motion is determined only modulo  $\pi$ , the recorded output voltage can be either positive or negative; see Fig. 3. The signature of this signal gives directly the collision rate of the electron with the background gas for encounters strong enough to induce a jump between the two possible phases. This mode is potentially useful in spin and  $g-2$  resonance experiments in which the electron is first spin polarized by exchange collisions with a polarized alkali beam and then analyzed on the basis of a difference between elastic singlet and triplet collision rates.<sup>1</sup>

Furthermore, since parametric excitation at  $2\nu_{z'}$  creates a regeneration band<sup>8</sup>  $\nu_{z'} - b < \nu_z < \nu_{z'} + b$  for harmonic oscillators of resonance frequency  $\nu_z$ , a bistable mode has been realized for  $0 < (\nu_{z'} - b) - \nu_{z0} \ll b$ , with  $b \propto u_{d0}$  and  $u_d = u_{d0} \cos 2\omega_z t$ . In the presence of the  $2\nu_{z'}$  drive the anharmonic<sup>9</sup> electron oscillator is either in state  $A$  at rest, or in state  $B$  carrying out an easily detectable driven oscillation at  $\nu_{z'}$  with a (large) amplitude shifting its resonant frequency to  $\nu_{z'} + b$ . Transition from state  $A$  to  $B$  may be triggered by any process transferring sufficient energy into the  $z$  motion to shift  $\nu_z$  from  $\nu_{z0}$  to  $>\nu_{z'} - b$ . This may, e.g., be accomplished by a gas collision when the cyclotron motion is sufficiently excited. This noise-free amplification scheme opens up ways for the detection of cyclotron, spin, and  $g-2$  resonances on a single electron or positron.

For appropriately miniaturized traps, our techniques may also be extended to single ions where direct detection of the axial as well as of the cyclotron motion (using a split-ring electrode)

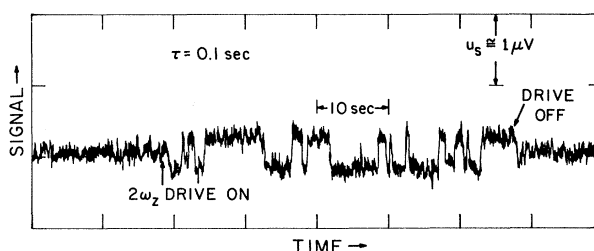


FIG. 3. Recorder trace of single-electron forced-oscillation signal at  $\nu_{z0} = 55.7$  MHz for parametric excitation at  $2\nu_{z0}$ . Gas collisions cause changes of the sign of the synchronously detected  $\nu_{z0}$  signal. The time constant  $\tau$  of the low-pass filter is much smaller than for Fig. 2.

is feasible. This should make possible cyclotron-resonance mass-spectroscopic studies of unprecedented resolution. For ions, the current record—a sensitivity to just detect a destructive transient four-ion signal in a Paul trap—is held by Rettinghaus.<sup>11</sup>

The inherent extreme sample economy should also be mentioned; e.g., it may be feasible to fill the effective trap volume with  $\sim 10^5$  molecules of a volatile compound like  $^{58}\text{Co}(\text{NO})(\text{CO})_3$  containing the positron emitter  $^{58}\text{Co}$  of  $\sim 70$  days half-life and to catch overnight one positron from the  $\sim 10^3$  radioactive events occurring during this period. The possibility of using the same positron or conceivably antiproton in a monoparticle oscillator over and over again in studies of *elastic* collisions with atomic partners provided by the background, atomic beams, or trapped ions is noted.

The apparatus was adapted from an earlier version originally built by Walls and Stein.<sup>5</sup>

\*Work supported by a grant from the National Science Foundation and U.S. Office of Naval Research contract; also in part by a grant from the U.S. Army Research Office.

<sup>1</sup>Compare H. Dehmelt, in *Advances in Atomic and Molecular Physics*, edited by D. R. Bates and I. Estermann (Academic, New York, 1967 and 1969), Vols. 3 and 5.

<sup>2</sup>Previously briefly reported in D. Wineland, P. Ekstrom, and H. Dehmelt, *Bull. Amer. Phys. Soc.* **18**, 785 (1973).

<sup>3</sup>S. Liebes and P. Franken, *Phys. Rev.* **116**, 633 (1959); H. Dehmelt and D. Wineland, *Bull. Amer. Phys. Soc.* (to be published).

<sup>4</sup>H. Dehmelt and P. Ekstrom, *Bull. Amer. Phys. Soc.* **18**, 727 (1973).

<sup>5</sup>F. Walls, Ph.D thesis, University of Washington,

1970 (unpublished); F. L. Walls and T. S. Stein, *Phys. Rev. Lett.* **31**, 975 (1973).

<sup>6</sup>See, e.g., W. Anderson, in *NMR and EPR Spectroscopy*, edited by Varian Associates (Pergamon, New York, 1960).

<sup>7</sup>H. Dehmelt and D. Wineland, *Bull. Amer. Phys. Soc.* **18**, 786 (1973).

<sup>8</sup>Compare L. D. Landau and E. M. Lifshitz, *Mechanics* (Pergamon, New York, 1960).

<sup>9</sup>N. Minorsky, *Nonlinear Oscillations* (Van Nostrand, Princeton, N.J., 1962).

<sup>10</sup>H. Dehmelt and P. Ekstrom, *Bull. Amer. Phys. Soc.* **18**, 408 (1973).

<sup>11</sup>G. Rettinghaus, *Z. Angew. Phys.* **22**, 321 (1967).

## Field Evaporation of Tungsten-Helium Molecular Ions

Erwin W. Müller, S. V. Krishnaswamy, and S. B. McLane

*Department of Physics, The Pennsylvania State University, University Park, Pennsylvania 16802*

(Received 20 September 1973)

Ions field evaporating from tungsten in the presence of helium are identified by a time-of-flight atom probe of improved resolution. Helium is found to be adsorbed at all imaged surface sites. From the brightly imaged crystal regions the adsorbate comes off as  $\text{He}^+$ , approximately in a one-to-one ratio with  $\text{W}^{+++}$  and  $\text{W}^{++++}$ . The dim, high work-function regions around (011) predominantly yield  $\text{WHe}^{+++}$  molecular ions with the temperature-dependent relative abundance peaking at liquid nitrogen temperature.

Field desorption<sup>1</sup> and field evaporation<sup>2</sup> are unique physical effects in which atoms are removed from a surface in a way entirely different from thermal evaporation or particle impact. The image-force theory<sup>1,2</sup> and Gomer's charge-exchange theory<sup>3</sup> describe the process fairly successfully, particularly when surface-atom polarizability and field penetration are taken into account.<sup>4,5</sup>

With the advent of the atom-probe field ion microscope (FIM) new information was obtained by the discovery of unexpected threefold and fourfold charges of field-evaporating metal ions,<sup>6,7</sup> of field adsorption of the noble imaging gases, and of the formation of metal-helium molecular ions.<sup>8,9</sup> While the high multiplicity of ionic charges still remains unexplained, field adsorption of noble gas ions can be quantitatively described by classical dipole-dipole interaction.<sup>10</sup> This bond suggests a position of the adsorbate at the apex of the kink-site atom, rather than at a recessed site as in ordinary adsorption. The apex position has been experimentally confirmed by localizing the origin of field-desorbing  $\text{He}^+$  and  $\text{Ne}^+$  within the forbidden zone through energy distribution measurements,<sup>11</sup> using excitation of the adsorbate by externally supplied slow electrons. Atom-probe investigations further demonstrated a correlation of regional image brightness with the appearance of field-desorbed  $\text{He}^+$  ions. In the bright regions of the FIM pattern of tungsten there is about one  $\text{He}^+$  ion desorbed for each field-evaporated metal

ion, while very few  $\text{He}^+$  ions are coming off in the dimly imaged region. McKinney and Brenner<sup>12</sup> also found this and reported the ratio of  $\text{He}^+/\text{W}^{+++}$  in the vicinity of (001) to be 0.03 only.

It appears that field ionization of the imaging gas is enhanced when the electron transition to the metal occurs through an already adsorbed noble gas atom.<sup>10,13</sup> The sharp localization of field ionization within a zone of only 0.2 Å depth as derived from energy distribution measurements<sup>14</sup> and the direct proof of enhanced field ionization through adsorbed Ne by Schmidt, Reiser, and Krautz<sup>15</sup> as well as by Rendulic,<sup>16</sup> and through adsorbed He by McLane, Müller, and Krishnaswamy<sup>17</sup> suggest that the apex adsorbate is of major importance for the FIM image information. It is now clear that earlier theoretical treatments of free-space field ionization near the surface are unrealistic. Nolan and Herman<sup>18</sup> have recently given the first quantum-mechanical calculation for field ionization through an apex-adsorbed gas atom using realistic atomic potentials.

However, it is not possible to explain the dim imaging of certain crystallographic regions by a low average degree of coverage with the He apex adsorbate as may be suggested by the observed low ratio of  $\text{He}^+/\text{W}^{+++}$ . There is ample supply of the gas, so that even with a locally smaller dipole binding energy in the low-field regions all sites should eventually be occupied when the temperature is lowered sufficiently.